Tractable Lensing Models For Testing IRS

Nikita Blinov and Cristiano Jose Franco Sampaio

Department of Physics and Astronomy, York University, Toronto, Ontario, M3J 1P3, Canada

July 30, 2024

Abstract

1 Introduction

Our goal is to produce a code to solve the lens equation

$$\boldsymbol{\beta} = \boldsymbol{\theta} - \boldsymbol{\alpha}(\boldsymbol{\theta}) \tag{1}$$

where $\boldsymbol{\beta}$, $\boldsymbol{\theta}$ are the angular positions of the source without and with deflection, and $\boldsymbol{\alpha}$ is the general-relativistic deflection which depends on the matter distribution in the lens. Many (local) properties of the lens map can be understood in terms of the Jacobian of the mapping $\boldsymbol{\beta}(\boldsymbol{\theta})$, $A \equiv \partial\boldsymbol{\beta}/\partial\boldsymbol{\theta}$ which is written as [1]:

$$A = \begin{pmatrix} 1-\kappa-\lambda & -\eta \\ -\eta & 1-\kappa+\lambda \end{pmatrix} \tag{2}$$

where κ, λ and η are the convergence and shear, which are naturally functions of θ (note that $A_{ij} = \delta_{ij} - \partial_i\alpha_j$). A is also called the (inverse) magnification matrix because the magnification of a source is given by the ratio of observed flux to unlensed flux[1]

$$\mu = \frac{Id^2\boldsymbol{\theta}}{Id^2\boldsymbol{\beta}} = |\partial\boldsymbol{\beta}/\partial\boldsymbol{\theta}|^{-1} = 1/\det A, \tag{3}$$

where $d^2\boldsymbol{\theta}$ and $d^2\boldsymbol{\beta}$ are area elements in the image and source planes, respectively. Regions for which $\det A = 0$ are critical curves in the lens plane and caustics in source plane.

In general there is no analytic solution for the image position as a function of the source position and the magnification. There are some symmetric situations that are tractable however, so we can use these to test our implementation of inverse ray shooting.

[1]The surface brightness I (flux density per solid angle) is the same for lensed and unlensed sources.

1.1 Schwarzchild Lens

This is the simplest example of all with a simple analytic solution: a spherical point lens at the origin for which the deflection is [2, 3]

$$\boldsymbol{\alpha}(\boldsymbol{\theta}) = \theta_E^2 \frac{\boldsymbol{\theta}}{\boldsymbol{\theta}^2} \tag{4}$$

where and $\theta_E = \sqrt{4GMD_{LS}/(D_L D_S)}$ is the characteristic angular scale (the Einstein radius) of the source-lens configuration. Now the lens equation is really two non-linear equations for two unknowns $\boldsymbol{\theta} = (\theta_1, \theta_2)$, but for axially symmetric configurations this can be reduced to a single non-linear equation without loss of generality: we can rotate the source-plane coordinates such that the source is at $\boldsymbol{\beta} = (\beta, 0)$, so that the lens equation implies that $\boldsymbol{\theta} = (\theta, 0)$, which simplifies it to a single equations

$$\beta = \theta - \frac{\theta_E^2}{\theta}. \tag{5}$$

This can be easily solved for the two image positions $\theta_\pm$

$$\theta_\pm = \frac{1}{2}\left(\beta \pm \sqrt{\beta^2 + 4\theta_E^2}\right) \tag{6}$$

From eq. (3) it follows that the magnifications of the two images are

$$\mu = \frac{\theta}{\beta}\frac{d\theta}{d\beta} \Rightarrow \mu_\pm = \frac{\theta_\pm^4}{\theta^4 - \theta_E^4} = \frac{u^2+2}{2u\sqrt{u^2+4}} \pm \frac{1}{2} \tag{7}$$

This means that for any position of the source β, we can analytically predict its image locations and their magnifications.

1.2 Singular Isothermal Sphere (SIS)

This is a model in which the mass of the lens is not concentrated at a single point, but rather has a (three-dimensional) distribution that goes like $1/r^2$ (note that there two "singularities"' here: the divergent density at the origin and that the total mass is infinite; these issues do not cause problems here because lensing is sensitive to the total mass within some radius, which is finite) [2, 3]. This is again an axially-symmetric situation (if the origin of the lens coincides with the origin of coordinates). The deflection angle is

$$\boldsymbol{\alpha}(\boldsymbol{\theta}) = \theta_E \frac{\boldsymbol{\theta}}{|\boldsymbol{\theta}|} \tag{8}$$

where $\theta = 4\pi\sigma_v^2 D_{LS}/D_S$ and σ_v is the velocity dispersion (a parameter of the density distribution). As for the Schwarzchild we can reduce the lens equation(s) to a single equation using circular symmetry.

$$\beta = \theta - \theta_E \frac{\theta}{|\theta|}. \tag{9}$$

(Note that here θ is defined through $\boldsymbol{\theta} = (\theta, 0)$ so it can be positive or negative). There are two solutions for the image positions:

$$\theta_\pm = \beta \pm \theta_E \tag{10}$$

while the magnifications are given by

$$\mu_\pm = 1 \pm \frac{\theta_E}{\beta} \tag{11}$$

Note that the solutions above exist when if $\theta_+ > 0$ or $\theta_- < 0$ (from expanding the absolute value in the lens equation); these constraints translate into $\beta > -\theta_E$ and $\beta < \theta_E$, respectively. This means that both solutions exist only when the source is within the Einstein radius of the lens.

1.3 Non-Singular Isothermal Sphere With External Shear

The previous examples were simple because of their circular symmetry. The caustic lensing we want to study is not as nice, so it is useful to have a less symmetric, but tractable case as well. One such example is described in [3], Ch. 3.4; it consists of two contributions to the lens equation: a circularly symmetric lens and an external shear, which is not circularly-symmetric.

The total deflection is

$$\boldsymbol{\alpha}(\boldsymbol{\theta}) = \frac{\theta_e}{\sqrt{\boldsymbol{\theta}^2 + \theta_c^2}} + \begin{pmatrix} \kappa_p + \gamma_p & 0 \\ 0 & \kappa_p - \gamma_p \end{pmatrix} \boldsymbol{\theta} \tag{12}$$

The first term here is the circularly-symmetric non-singular isothermal sphere with $\theta_{e,c}$ being parameters of the system (note the similarity to eq. (8) as $\theta_c \to 0$); the second term is the external shear, or "quadrupole" lens - it is not spherically symmetric.

To get some analytic insight we again need to reduce this problem to a single equation. After some manipulations (and source-plane variable rescalings) the lens equation becomes

$$\boldsymbol{\beta} = \begin{pmatrix} 1 - g_p & 0 \\ 0 & 1 + g_p \end{pmatrix} \boldsymbol{\theta} - \bar{\kappa}(|\boldsymbol{\theta}|)\boldsymbol{\theta}, \tag{13}$$

where $\bar{\kappa}(\theta) = \theta_e(1-\kappa_p)^{-1}/\sqrt{\theta^2 + \theta_c^2}$, $g_p = \gamma_p/(1-\kappa_p)$ and $\boldsymbol{\beta} = \boldsymbol{\beta}_{\text{original}}/(1-\kappa_p)$. Next, we use polar coordinates $\boldsymbol{\theta} = \theta(\cos\varphi, \sin\varphi)$ in the lens plane to rewire the components of the lens equation as

$$\cos\varphi = \frac{\beta_1}{\theta(1 - g_p - \bar{\kappa}(\theta))}, \quad \sin\varphi = \frac{\beta_2}{\theta(1 + g_p - \bar{\kappa}(\theta))}. \tag{14}$$

These two equations can be squared and summed to yield a single equation:

$$\theta^2 \left[(1-\bar{\kappa}(\theta))^2 - g_p^2\right]^2 - \beta_1^2(1 - \bar{\kappa}(\theta) + g_p)^2 - \beta_2^2(1 - \bar{\kappa}(\theta) - g_p)^2 = 0 \tag{15}$$

Since $\bar{\kappa}(\theta)$ is a known function, this is a single equation for the radial position(s) of the images of the source at $\boldsymbol{\beta} = (\beta_1, \beta_2)$. One can show that this is a sixth order polynomial, so we can solve it numerically to find any real roots. One then needs to plug them back into eq. (14) and check whether $|\cos\varphi|,\ |\sin\varphi| \leq 1$.

1.4 Lensing Near a Fold Caustic

Galaxy cluster lenses are complicated, so the global caustic structure is also complicated – see Fig. 1 in [4]. There is, however, a huge simplification: since are interested in observing individual stars that live very close a specific stretch of the caustic, we should be able to approximate the caustic by a line segment. To make this intuition concrete we start with the Fermat potential formulation of the lensing problem. The lens equation can be written as (see Sec. 3.3 in [2])

$$\nabla_\theta \left(\frac{1}{2}(\boldsymbol{\theta} - \boldsymbol{\beta})^2 - \psi(\boldsymbol{\theta}) \right) = 0 \tag{16}$$

where ψ is the effective lensing potential:

$$\psi(\boldsymbol{\theta}) = \frac{1}{\pi} = \int d^2\theta' \kappa(\boldsymbol{\theta'}) \ln|\boldsymbol{\theta} - \boldsymbol{\theta'}| \tag{17}$$

such that $\nabla_\theta \psi = \boldsymbol{\alpha}(\boldsymbol{\theta})$. Here $\kappa(\boldsymbol{\theta})$ is called the convergence; it is just a rescaled projected matter density:

$$\kappa = \frac{1}{\Sigma_{cr}} \int \rho(\boldsymbol{\theta}, z) dz, \;\; \Sigma_{cr} = \frac{c^2}{4\pi G} \frac{D_S}{D_L D_{LS}} \tag{18}$$

(Note Σ_{cr} is a number that is specific to each system that is observed).

The quantity in the parentheses of eq. (16), called the Fermat potential:

$$\phi \equiv \frac{1}{2}(\boldsymbol{\theta} - \boldsymbol{\beta})^2 - \psi(\boldsymbol{\theta}) \tag{19}$$

This has a nice physical interpretation: it is proportional to the time delay function...(expand on this - NB)

For the galaxy cluster the lens problem is complicated because the matter distribution ρ and the resulting convergence κ and lens potential ψ are complicated. By focusing on a small region of the lens we can Taylor expand the Fermat potential (see Ch. 6.2 in [3]); the expansion is around $\boldsymbol{x}^{(0)}$, $\boldsymbol{y}^{(0)}$, such that the coordinated $\boldsymbol{x}$, $\boldsymbol{y}$ measure the deviations from them. The resulting expansion looks like

$$\phi \approx \phi^{(0)} + \frac{1}{2}\boldsymbol{y}^2 - \boldsymbol{x}\cdot\boldsymbol{y} + \frac{1}{2}\boldsymbol{x}^2 + (\boldsymbol{x}^{(0)} - \boldsymbol{y}^{(0)})\cdot(\boldsymbol{x} - \boldsymbol{y}) - \psi_1^{(0)} x_1 - \psi_2^{(0)} x_2 - \frac{1}{2}\psi_{11}^{(0)} x_1^2 - \frac{1}{2}\psi_{22}^{(0)} x_2^2 - \psi_{12}^{(0)} x_1 x_2 + \ldots \tag{20}$$

where the subscripts $1, 2$ indicate derivatives with respect to $x_{1,2}$; the superscript indicates that the quantity is evaluated at $\boldsymbol{x}^{(0)}$ and the dots stand for higher derivatives.

This expansion is general, but we want to focus on regions of the lens/source plane very close to the cluster critical/caustic curve. Specifically, let us assume that our expansion point $\boldsymbol{x}^{(0)}$ ($\boldsymbol{y}^{(0)}$) lies on the critical curve (caustic). This imposes restrictions on the various derivatives of the Fermat potential, since we know that

$$0 = \det A_{ij}^{(0)} = \det \phi_{ij}^{(0)} \Rightarrow \phi_{11}\phi_{22} - \phi_{12}^2 = 0. \tag{21}$$

Note that this means that $A_{ij}^{(0)}$ has at least one zero eigenvalue; the case with exactly one zero eigenvalue gives rise to a "fold" caustic; two zero eigenvalues give rise to more complicated caustics. We make additional assumptions to reduce the number of constants we need to consider: since $A_{ij}^{(0)}$ is a real symmetric matrix, we can perform diagonalize it with a coordinate rotation, such that

$$A_{ij}^{(0)} = \begin{pmatrix} \phi_{11} & 0 \\ 0 & \phi_{22} \end{pmatrix}, \tag{22}$$

that is we are setting $\phi_{12}^{(0)} = -\psi_{12}^{(0)} = 0$. Since one of the eigenvalues must be 0, we must have $\phi_{11}^{(0)} = 0$ or $\phi_{22}^{(0)} = 0$ (but not both at the same time!) This last condition implies that

$$1 - \psi_{11}^{(0)} = 0 \text{ OR } 1 - \psi_{22}^{(0)} = 0 \tag{23}$$

The two choices correspond to different orientations of the critical curve in the lens plane. Finally, since the pair of points $\boldsymbol{x}^{(0)}$, $\boldsymbol{y}^{(0)}$ satisfy the lens equation, there are two more constraints:

$$0 = \phi_i^{(0)} = x_i^{(0)} - y_i^{(0)} - \psi_i^{(0)} \tag{24}$$

With these additional constraints the Fermat potential becomes

$$\phi \approx \phi^{(0)} + \frac{1}{2}\boldsymbol{y}^2 - \boldsymbol{x}\cdot\boldsymbol{y} + \frac{1}{2}\phi^{(0)}_{11}x_1^2 + \frac{1}{2}\phi^{(0)}_{22}x_2^2 + \frac{1}{6}\phi^{(0)}_{111}x_1^3 + \frac{1}{6}\phi^{(0)}_{222}x_2^3 + \frac{1}{2}\phi^{(0)}_{112}x_1^2x_2 + \frac{1}{2}\phi^{(0)}_{122}x_1x_2^2. \quad (25)$$

From this we can derive the lens mapping (dropping the $^{(0)}$ superscript on expansion coefficients)

$$y_1 = \frac{x_1^2\phi_{111}}{2} + x_1x_2\phi_{112} + x_1\phi_{11} + \frac{x_2^2\phi_{122}}{2}, \quad (26)$$

$$y_2 = \frac{x_1^2\phi_{112}}{2} + x_1x_2\phi_{122} + \frac{x_2^2\phi_{222}}{2} + x_2\phi_{22} \quad (27)$$

and the Jacobian

$$A = \begin{pmatrix} x_1\phi_{111} + x_2\phi_{112} + \phi_{11} & x_1\phi_{112} + x_2\phi_{122} \\ x_1\phi_{112} + x_2\phi_{122} & x_1\phi_{122} + x_2\phi_{222} + \phi_{22} \end{pmatrix} \quad (28)$$

For now let us specialize to the case that $\phi_{11} \neq 0$ and $\phi_{22} = 0$. By computing $\det A$ and assuming x_i are small, we find that

$$0 = \det A \Rightarrow x_2 = -\frac{\phi_{122}}{\phi_{222}}x_1. \quad (29)$$

This tells us that the critical curve in the image plane is a straight line passing through the origin with slope determined by the third derivatives of the Fermat potential. By solving the lens mapping along the critical curve for y_1, y_2 (i.e., plug the critical curve into the lens map, eliminating x_1 in favour of y_1 defines a relation $y_2(y_1)$) one can show that the caustic is a parabola in the source plane.

What values do we choose for the Fermat potential derivatives? We can relate them to quantities that have been extracted from models of real galaxy clusters [5]. This paper actually provides the code and the lens models needed to compute the various derivatives of the Fermat potential at the source positions. They use a slightly different notation (one that is consistent with [4, 6]) so we need to map their results onto ϕ_{111}, ϕ_{112}, etc. They write the magnification matrix as

$$A = \begin{pmatrix} 1 - \kappa - \lambda & -\eta \\ -\eta & 1 - \kappa + \lambda \end{pmatrix} \quad (30)$$

At the critical curve $1 - \kappa - \lambda$ vanishes and $1 - \kappa + \lambda$ becomes the non-zero eigenvalue; the coordinates are rotated such that η vanishes on the critical curve just like we did above. Note that eq. (30) specializes to the coordinate choice where the first eigenvalue vanishes on the critical line, whereas eq. (28) is can be adapted to both choices, depending on whether $\phi_{11} = 0$ or $\phi_{22} = 0$. For $\phi_{11} = 0$ the mapping between the two notations is

$$-\nabla(\kappa + \lambda) = (\phi_{111}, \phi_{112}), \quad \phi_{22} = 2(1 - \kappa_0), \quad \nabla(-\kappa + \lambda) = (\phi_{122}, \phi_{222}), \quad -\nabla\eta = (\phi_{112}, \phi_{122}). \quad (31)$$

For the other choice, $\phi_{22} = 0$ we have

$$-\nabla(\kappa + \lambda) = (\phi_{122}, \phi_{222}), \quad \phi_{11} = 2(1 - \kappa_0), \quad \nabla(-\kappa + \lambda) = (\phi_{111}, \phi_{112}), \quad -\nabla\eta = (\phi_{112}, \phi_{122}). \quad (32)$$

1.4.1 Physically Motivated Parameters

Using the code provided by [5] we can estimate the sizes of the various derivatives for several highly magnified stars and different lens models. The summary is that the gradients in the previous equations at the locations of the highly magnified stars have typical magnitudes of few $\times$ arcmin^{-1}, while the separation of the image from the critical line (i.e. typical values of $x_{1,2}$) are $\lesssim$ arcsec. Typical values of κ_0 are 0.4-0.9. These results are summarized in table 1 for a few stars. Note that this provides some validation for the Taylor expansion of the lens mapping that we started with in eq. (27): terms like $\phi_{111}x_1 \sim 10^{-2}$ are small compared to $\phi_{11} = 2(1-\kappa_0)$; this also justifies dropping terms like $(\phi_{111}x_1)^2$ when deriving the shape of the critical line in eq. (29).

2 Modelling Random Density Fluctuations

We want to add a term to our lens map that represents small-scale fluctuations of the DM density due to the presence of randomly-distributed DM clumps called minihalos. With this goal in mind we decompose the lensing deflection into a smooth component (what we have been modelling so far) $\boldsymbol{\alpha}_S$ and a stochastic fluctuation $\delta\boldsymbol{\alpha}$:

$$\boldsymbol{\alpha} = \boldsymbol{\alpha}_S + \delta\boldsymbol{\alpha}. \tag{33}$$

While the precise positional dependence of $\delta\alpha$ is impossible to know (the DM is clumps are distributed randomly and are constantly shifting around), the statistical properties of $\delta\alpha$ (i.e. which distribution it is drawn from) can be related to a DM model by recalling the relation of the lensing deflection and the matter density in the lens:

$$\delta\boldsymbol{\alpha} = \frac{1}{\pi}\int d^2x' \delta\kappa(\boldsymbol{x}')\frac{\boldsymbol{x}-\boldsymbol{x}'}{|\boldsymbol{x}-\boldsymbol{x}'|^2}. \tag{34}$$

Here $\delta\kappa$ are the fluctuations in the lensing convergence, i.e. projected/surface mass density fluctuation [6] from eq. (18)

$$\delta\kappa(\boldsymbol{x}) = \frac{1}{\Sigma_{cr}}\int_{\text{l.o.s.}} \delta\rho(\boldsymbol{x}, z)dz \tag{35}$$

where the z integration is over the line of sight to the source and the normalization factor Σ_{cr} is the critical surface mass density:

$$\Sigma_{cr} = \frac{c^2 D_S}{4\pi G D_L D_{LS}} = 1660 M_\odot/\text{pc}^2 \times \frac{1\text{ Gpc}}{D_L D_{LS}/D_S} \tag{36}$$

These definitions ensure that $\delta\kappa$ is dimensionless. In absence of the smooth lens, if $\delta\kappa$ is small, then the lensing effects are small.

A simple physical model for $\delta\kappa(\boldsymbol{x})$ is a 2D Gaussian random field. This means that the value of $\delta\kappa$ at any $\boldsymbol{x}$ is a random number, but there is a known correlation between nearby points. "Gaussian" simply means that all correlations can be expressed in terms of the two-point correlation function. This discussion is much more clear in Fourier space, which also explains how we can generate random realizations of $\delta\kappa$ and therefore of $\delta\boldsymbol{\alpha}$.

Rewriting the deflection in terms of Fourier transforms we find

$$\delta\boldsymbol{\alpha}(\boldsymbol{x}) = \frac{1}{\pi}\int \frac{d^2\ell}{(2\pi)^2}\left(\frac{2\pi i\boldsymbol{\ell}}{\ell^2}\right)\delta\kappa(\boldsymbol{\ell})e^{-i\boldsymbol{x}\cdot\boldsymbol{\ell}} \tag{37}$$

Name	$\lvert\Delta\boldsymbol{x}\rvert$ (arcsec)	κ_0	$-\nabla(\kappa+\lambda)$ [arcmin^{-1}]	$\nabla(-\kappa+\lambda)$ [arcmin^{-1}]	$\nabla\eta$ [arcmin^{-1}]
LS1 (Icarus) lensed by MACSJ1149 (Kelly 2018)	0.138	0.832	$[-4.511, 1.681]$	$[-0.87, 2.096]$	$[-1.831, 0.083]$
LS2 (NW Spock) lensed by MACSJ0416 (Rodney 2018)	0.485	0.742	$[5.315, 2.209]$	$[1.804, 0.123]$	$[-0.11, -0.805]$
LS3 (SE Spock) lensed by MACSJ0416 (Rodney 2018)	1.396	0.629	$[5.315, 2.209]$	$[1.804, 0.123]$	$[-0.11, -0.805]$
LS4 (Warhol) lensed by MACSJ0416 (Kaurov 2019 / Chen 2019)	0.183	0.686	$[-6.848, 0.276]$	$[0.941, -1.914]$	$[3.576, -1.432]$
LS5 (Earendel) lensed by WHL0137 (Welch 2022)	0.164	0.590	$[-0.719, -2.358]$	$[0.559, -0.985]$	$[0.657, 0.616]$
LS7 (...) lensed by Abell 2744 (Chen 2022)	0.158	0.726	$[3.821, -0.197]$	$[0.173, 6.109]$	$[-1.339, 0.611]$
LS8 (star-1) lensed by MACSJ0647 (Meena 2023)	0.683	0.544	$[-2.027, 0.295]$	$[0.408, 0.249]$	$[-0.182, -0.603]$
LS9 (star-2) lensed by MACSJ0647 (Meena 2023)	0.488	0.549	$[-1.937, 0.312]$	$[0.363, 0.263]$	$[-0.224, -0.519]$
LS10 (Quyllur) lensed by El Gordo (Diego 2023)	0.977	0.662	$[1.208, 2.208]$	$[-0.12, 0.638]$	$[0.826, 0.771]$
LS11 (...) lensed by Abell 370 (Meena 2023)	0.785	0.703	$[-3.164, -0.2]$	$[0.514, -1.941]$	$[0.58, 0.053]$
LS12 (Mothra) lensed by MACSJ0416 (Diego 2023)	0.553	0.936	$[-3.786, 0.357]$	$[-2.933, 0.071]$	$[0.374, -0.424]$

Table 1: Table of gradients and other values needed to evaluate the lens map and the magnification matrix in the near-critical-line expansion. Each line corresponds to a different image, and the various parameters were derived using the code provided with [5]; when multiple lens models were available, the results were simply averaged. (THIS TABLE NEEDS TO BE CORRECTED - THE CRITICAL LINES ARE NOT ALIGNED CORRECTLY - NB)

where $\boldsymbol{\ell}$ is the Fourier conjugate variable to $\boldsymbol{x}$. In the parentheses we have the Fourier transform of $(\boldsymbol{x}-\boldsymbol{x}')/(|\boldsymbol{x}-\boldsymbol{x}'|^2)$; $\delta\kappa(\boldsymbol{\ell})$ is the Fourier transform of $\delta\kappa(\boldsymbol{x})$. The Gaussian random field assumption means that $\delta\kappa(\boldsymbol{\ell})$ are random numbers drawn from a Gaussian distribution with a known variance; in the continuum limit each $\boldsymbol{\ell}$ corresponds to a different random number, but in a computer simulation there will be a finite number of them. The advantage of working in Fourier space is that these random numbers are not correlated - that is if we have N discrete ℓ values, we can draw N independent samples from different Gaussian distribution and then compute the discrete analogue of eq. (37).

What are the variances of the normal distribution from which we sample $\delta\kappa(\boldsymbol{\ell})$? We can schematically represent the sampling procedure as

$$\delta\kappa(\ell) \sim \frac{1}{\sqrt{2\pi P_\kappa(\ell)}} \exp\left(-\frac{\delta\kappa(\ell)^2}{2P_\kappa(\ell)}\right) \tag{38}$$

where the variance of the Gaussian (usually called σ^2) is called $P_\kappa(\ell)$, the power spectrum. It is P_κ that we can often predict from some model of DM. Often P_κ peaks at some value of ℓ which suggests that there is a lot of structure with characteristic angular size $1/\ell$.

An example power spectrum is shown in fig. 1. The assumptions that go into these power spectra are that DM is composed of DM minihalos of equal mass, with with a certain density profile called NFW.

The strategy for generating different realizations of $\delta\boldsymbol{\alpha}$ for a given DM model (e.g., the one in fig. 1) is as follows

1. Starting with a discrete grid of $\boldsymbol{\ell}$ values, generate a $\delta\kappa(\ell)$ by sampling from a Gaussian of appropriate variance, i.e. via eq. (38).
2. Compute the Fourier coefficient of $\delta\boldsymbol{\alpha}$ via eq. (37):
$$\delta\boldsymbol{\alpha}(\boldsymbol{\ell}) = \frac{2i\boldsymbol{\ell}}{\ell^2}\delta\kappa(\ell) \tag{39}$$
3. Invert the discrete Fourier transform to compute $\delta\boldsymbol{\alpha}(\boldsymbol{x})$ from $\delta\boldsymbol{\alpha}(\boldsymbol{\ell})$

References

[1] J. Miralda-Escude, *The Magnification of Stars Crossing a Caustic. I. Lenses with Smooth Potentials*, ApJ **379** (Sept., 1991) 94.

[2] R. Narayan and M. Bartelmann, *Lectures on gravitational lensing*, in *13th Jerusalem Winter School in Theoretical Physics: Formation of Structure in the Universe*, 6, 1996. astro-ph/9606001.

[3] P. Schneider, G. Meylan, C. Kochanek, P. Jetzer, P. North and J. Wambsganss, *Gravitational Lensing: Strong, Weak and Micro: Saas-Fee Advanced Course 33*. Saas-Fee Advanced Course. Springer Berlin Heidelberg, 2006.

[4] T. Venumadhav, L. Dai and J. Miralda-Escudé, *Microlensing of Extremely Magnified Stars near Caustics of Galaxy Clusters*, *Astrophys. J.* **850** (2017) 49, [1707.00003].

[5] C. V. Müller and J. Miralda-Escudé, *Limits on Dark Matter Compact Objects implied by Supermagnified Stars in Lensing Clusters*, 2403.16989.

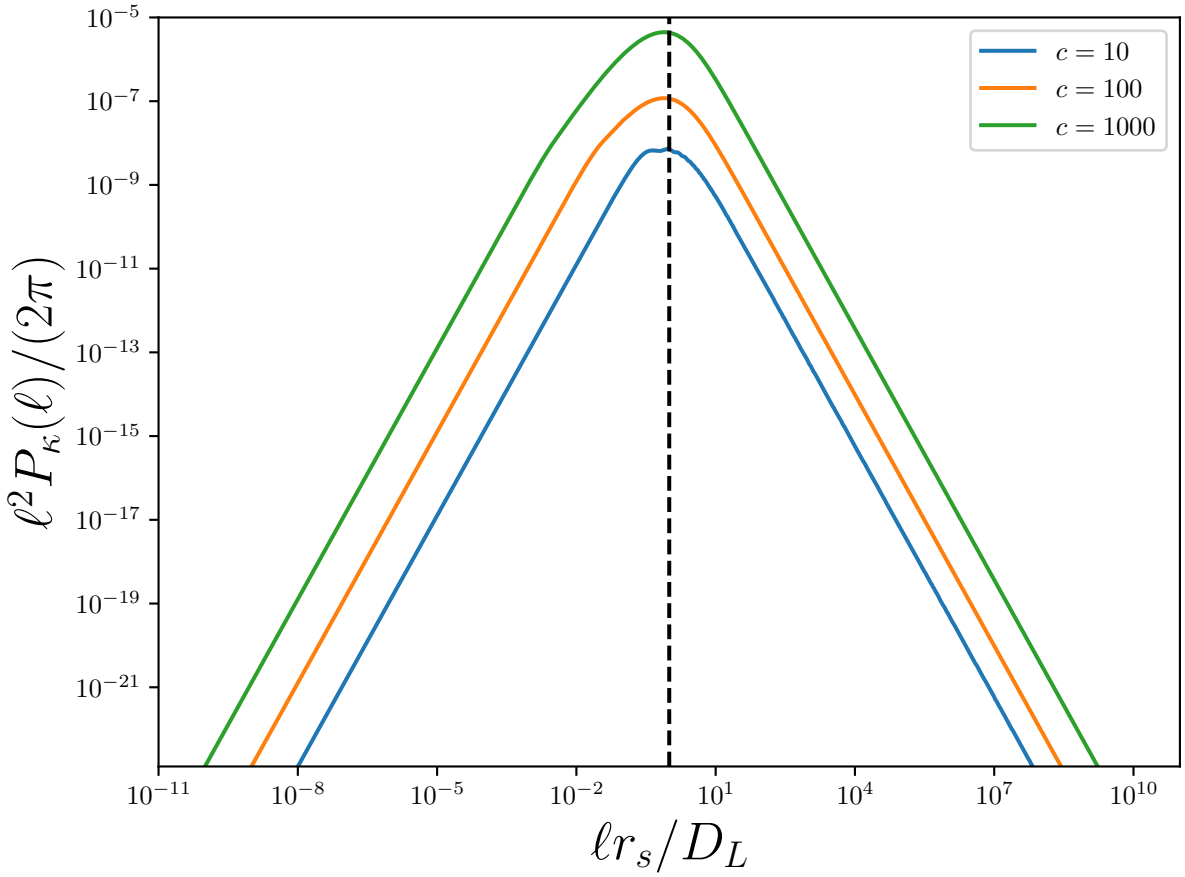

Figure 1: Example of a convergence power spectrum (with some rescaling factors) for a model of DM consisting of minihalos of fixed mass ($10^{-6} M_\odot$) and with different concentration parameters c (this parameter sets how dense these objects are). Other parameters are chosen to be $D_L = 1.35$ Gpc, $D_S = 1.79$ Gpc, $D_{LS} = 0.95$ Gpc, corresponding to [7].

[6] L. Dai and J. Miralda-Escudé, *Gravitational Lensing Signatures of Axion Dark Matter Minihalos in Highly Magnified Stars*, 1908.01773.

[7] P. L. Kelly et al., *Extreme magnification of an individual star at redshift 1.5 by a galaxy-cluster lens*, *Nature Astron.* **2** (2018) 334–342, [1706.10279].